Single-electrolyte isotachophoresis : on-chip analyte focusing and separation

Quist, J.W.

2 Electric Field Gradient Focusing = Isotachophoresis: a Review

A revised version of this chapter has been submitted as a Perspective article to the journal Analytical Chemistry

Isotachophoresis (ITP) and electric field gradient focusing (EFGF) are two powerful approaches for simultaneous focusing and separation of charged compounds. In EFGF, ionic analytes are immobilized on an electric field gradient, implying that, as in ITP, all focused analytes migrate with the same velocity upon completion of the separation. Therefore we argue in this review that EFGF methods should be regarded as forms of ITP. This claim is supported by theoretical and experimental studies from literature where EFGF demonstrates isotachophoretic hallmarks, including observations of plateau concentrations and contiguous analyte bands. An important implication of this unification is that functionality and applications developed on one platform can be transferred to other platforms. Single-electrolyte isotachophoretic separations with tunable ionic mobility window can be performed, as is illustrated with the example of depletion zone isotachophoresis (dzITP). We foresee many interesting combinations of ITP and EFGF features, yielding powerful analytical platforms for biomarker discovery, molecular interaction assays, drug screening and clinical diagnostics.

Isotachophoresis (ITP) and electric field gradient focusing (EFGF) are two classes of methods which are capable of simultaneous analyte separation and

efficient focusing. Concentration factors often exceed thousandfold and sometimes even millionfold for both ITP[1-3] and EFGF methods[4-9]. We believe that these similarities between ITP and EFGF are no coincidence. This review aims to provide a conceptual framework and to discuss experimental support for the unification of ITP and EFGF. As ITP is one of the most difficult to understand among electrokinetic techniques, we will first discuss the basic principles of this powerful method. Next, EFGF and the many variants thereof will be introduced, including conductivity gradient focusing (CGF), temperature gradient focusing (TGF), dynamic field gradient focusing (DFGF), electrocapture (EC), bipolar electrode focusing (BEF) and micro/nanofluidic concentration polarization (CP) devices. We then present our arguments for regarding EFGF techniques as forms of ITP and vice versa and provide support from several previous studies. Finally, we discuss the opportunities for different application areas in the life sciences created by the synergism of integrated ITP/EFGF platforms.

This review aims at understanding rather than comprehensiveness. Since the year 2000, numerous general reviews on electrokinetic preconcentration methods have been published[10-28]. These reviews include stacking methods like field amplified sample stacking/injection (FASS, FASI) and micellar methods like sweeping and micellar affinity gradient focusing (MAGF), which will not be considered here. For ITP, several useful introductory reviews are available[29-31], while updates on recent developments have been frequently given by Gebauer et al[32-38]. For EFGF technologies, the review by Shackmann and Ross provides an excellent introduction[39], but several more reviews are available[40-43].

Isotachophoresis

The isotachophoretic condition

The word "isotachophoresis" contains the Greek words isos (equal) and takhos (speed), capturing the essence of the method: an ITP separation is forced towards a dynamic equilibrium in which all co-ions migrate with the same velocity. The electrophoretic velocity v_i of an ion is determined by its ionic mobility μ_i and by the local electric field E:

$$v_i = \mu_i E \qquad (1)$$

Therefore, if ions with different ionic mobilities have the same velocity they must be in regions with different local electric fields. Under the isotachophoretic condition that all co-ions migrate with same velocity, each co-ion must be situated in its own zone in which the electric field exactly matches the ionic mobility of the co-ion. In other words, ions a, b and c with ionic mobilities $\mu_a < \mu_b < \mu_c$ will appear in zones A, B and C in which

$$\mu_{a,A} E_A = \mu_{b,B} E_B = \mu_{c,C} E_C \qquad (2)$$

Ionic mobilities are influenced by factors that may vary from zone to zone like pH and ionic strength, hence the zone subscripts A, B and C.

Disturbances of the isotachophoretic condition are subjected to a self-correcting mechanism (figure 1). If any ion with mobility μ_b were transported to zone C (for example, by diffusion) the lower electric field would cause it to migrate with lower velocity than all the surrounding ions with higher mobility μ_c, until it returns in zone B.

Inversely, if the same ion would be placed in zone A, it would encounter higher electric field and would move faster than the surrounding ions with lower mobility μ_a, again bringing the ion back in zone B. This self-correcting mechanism makes that in isotachophoresis pure co-ion zones are formed with

sharply defined borders. The sharpness of these borders is determined by a balance of electromigration and dispersion: at lower electric fields diffusion is more dominant, while higher electric fields lead to sharper zones.

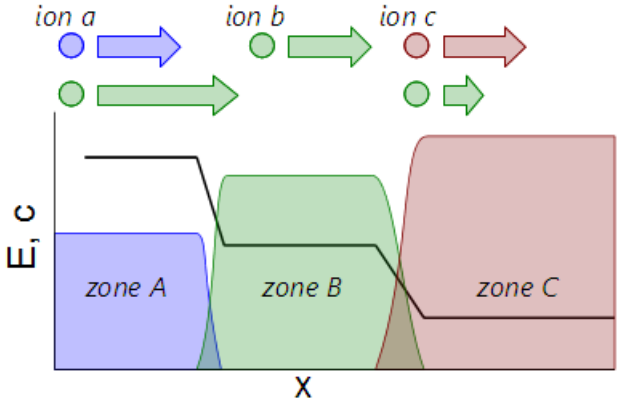

Figure 1. Self-correcting mechanism in ITP. Arrows represent electrophoretic velocities of ions. Profiles of electrical field and ion concentration profiles are indicated in the graph.

Plateau concentrations

Ion concentrations directly influence conductivity and local electric field. Therefore, each isotachophoretic zone must not only have its own electric field, but also must reach a corresponding plateau concentration (there is an exception for analytes in trace quantities, which will be discussed as "peak mode ITP" below). We assume monovalent strong ions, a common counterion x, and pure isotachophoretic zones. Under these conditions electroneutrality dictates:

$$c_{a,A} = c_{x,A} \qquad (3)$$

$$c_{b,B} = c_{x,B} \qquad (4)$$

For separations in linear channels, the current in all zones is equal ($I_A = I_B$). Therefore, considering only zones A and B:

$$\sum_i c_{i,A}\mu_{i,A}E_A A_A = \sum_i c_{i,B}\mu_{i,B}E_B A_B \qquad (5)$$

where A is the cross section of the channel. As we deal with pure zones, we only have to sum the co-ion and the common counterion *x*. Therefore, assuming uniform cross section we have

$$c_{a,A}\mu_{a,A}E_A + c_{x,A}\mu_{x,A}E_A = c_{b,B}\mu_{b,B}E_B + c_{x,B}\mu_{x,B}E_B \qquad (6)$$

which using eq 3 and 4 simplifies to

$$c_{a,A}(\mu_{a,A} + \mu_{x,A})E_A = c_{b,B}(\mu_{b,B} + \mu_{x,B})E_B \qquad (7)$$

Invoking the isotachophoretic condition in eq 2 results in

$$c_{b,B} = c_{a,A}\frac{(\mu_{a,A} + \mu_{x,A})\mu_{a,A}}{(\mu_{b,B} + \mu_{x,B})\mu_{b,B}} \qquad (8)$$

This equation tells that the plateau concentration $c_{b,B}$ of ion b in zone B is in principle solely dependent on the concentration $c_{a,A}$ of ion a in zone A and on the mobilities of the ions involved. Eq 8 also may be derived from the Kohlrausch regulation function (KRF)[44]:

$$KRF = \sum_i \frac{z_i c_i}{\mu_i} \qquad (9)$$

The KRF is a conservation law: at each position in any electrokinetic separation the value for KRF remains constant over time. If a bulk flow is present, KRF moves with the flow.

The importance for ITP is that the KRF remains the same even after an analyte or trailing electrolyte zone has replaced a leading electrolyte zone, dictating the concentrations in these zones. A clear and more extensive discussion of the KRF and its limitations, and of other conservation laws in electrophoresis has been provided by Hruška and Gaš[45].

Leading and trailing electrolytes

From the isotachophoretic condition we have deduced a number of important hallmarks of ITP separations: the formation of pure zones with sharply defined borders, a self-correcting mechanism, and plateau concentrations. This isotachophoretic condition can be imposed on a separation by introducing a discontinuous electrolyte system which contains at least a high-mobility leading electrolyte (LE) and a low-mobility trailing electrolyte (TE). The TE cannot move faster than the LE and overcome it, because the LE ions have higher mobility. The TE can neither move slower in the sense that an electrolyte-free zone would form between the TE and the LE, because such a region would be rapidly filled with TE ions by the increased electric field. The TE and LE zones therefore must move with equal velocity. Electric field in the TE becomes adjusted accordingly while the TE concentration is adjusted by Kohlrausch regulation.

Analytes, spacers and tracers

Since ITP has a self-correcting mechanism, analyte injection can take place by dissolution in the TE or in the LE. Usually, TE injections are preferred because the higher electric field in the TE speeds up the ITP process. The TE and the LE define an ionic mobility window. Analytes within the ionic mobility window will migrate towards the LE/TE interface and will be focused there. Ions with higher mobilities than the LE or lower mobilities than the TE will be transported away from the LE/TE interface. Focused analytes migrate with the same velocity as the LE and TE ions, fulfilling the isotachophoretic condition. The analytes will form contiguous plateau zones that are ordered according their ionic mobilities. The electric fields and the conductivities in the zones

will form a stair-like profile, the lowest electric field and highest conductivity being situated in the LE zone.

In order to achieve baseline separation between two adjacent analyte zones, spacers can be used. A spacer is an ion that has intermediate mobility between two analytes and therefore will insert between the two analyte zones and space them apart. For example, non-fluorescent spacers may be used to make two adjacent fluorescent zones discernable. Similarly, fluorescent spacers can be used for indirect detection and quantification of plateau zones of non-fluorescent analytes.[46]

Tracers aid in visualization of ITP zones. Tracer ions are continuously supplied in low concentrations to prevent significant alterations of the ITP process. While migrating through the ITP zones, tracer ions undergo stacking due to the differences in local electric field. In other words, the tracer concentration co-adjusts to the local conductivity. This enables visualization of different zones. Chambers et al. distinghuished three kinds of tracer: so-called counterspeeders, underspeeders and overspeeders[47]. Counterspeeders are counterionic tracers, which migrate in opposite direction as the ITP zones. Underspeeders and overspeeders are co-ionic tracers which have respectively lower and higher mobility than all relevant analytes. As a tool for indirect detection, tracers are an interesting alternative to fluorescent labels and intercalating dyes.

Peak mode and plateau mode

ITP separations often can be readily recognized by a stairlike profile of contiguous plateau-shaped analyte zones. In simple cases, plateau concentrations can be predicted from the leading electrolyte concentration

and the mobilities of the analyte ion, the counterion and the leading ion (eq 8). However, in many cases analytes have insufficient quantities to reach plateau concentrations. Such analytes will form focused peaks between the zones of the ions with the nearest mobilities. This situation is often referred to as "peak mode ITP" and is contrasted to "plateau mode ITP"[48]. In principle, at the start of an ITP separation every analyte zone starts as a peak.

Overlap between adjacent ITP zones is always present due to diffusion. The concentration gradients in these overlap regions provide an electric field gradient on which analytes with intermediate mobilities find a focusing position. During the transition from peak mode to plateau mode, the focusing analytes replace co-ions at the same positions, gradually flattening the electric field gradient. When all co-ions are replaced, the focusing analyte has reached plateau concentration.

The overlap between zones, which is particularly strong in peak mode ITP, limits the capacities of ITP for separation purposes. For example, Kaniansky et al.[49] demonstrated an ITP separation of 14 small molecules, which is a fairly large number for an ITP separation. This is in contrast to zone electrophoresis, where electropherograms may show hundreds of peaks. To increase separation efficiency ITP is often combined with zone electrophoresis by means of transient ITP (see next section). Zone overlap also can be used very advantageously. Bercovici et al. showed that hybridization of two different DNA strands could be accelerated over 10 000 fold by means of peak mode ITP because of the ability to concentrate the DNA molecules in a very confined volume.[50]

The plateau concentrations resulting from Kohlrausch regulation impose a limit to analyte preconcentration. Nevertheless, if analytes have very low

starting concentrations and sufficient time is provided, peak mode ITP can be used to obtain extremely high concentration factors. Several articless report over 10000-fold protein preconcentration[2, 3, 51], and in ideal conditions, millionfold concentration of a fluorophore has been achieved.[1]

Non-equilibrium ITP processes

The isotachophoretic condition only holds for completed ITP separations. There are several situations in which the dynamic equilibrium, which is associated with the isotachophoretic condition, is never reached. Incomplete ITP separations are characterized by the presence of mixed zones, which contain multiple co-ions with different mobilities. For example, sample might be injected continuously, resulting in continuously broadening zones. A well-known non-equilibrium ITP process is transient ITP (tITP). Several tITP alternatives exist[52]. For example, analytes are dissolved in a TE plug which is sandwiched between LE zones. The analytes are focused at the front end of the TE plug, while the back of the TE plug is dissolved by the faster LE ions. When the TE becomes completely dissolved, ITP focusing ceases and analytes are separated by zone electrophoresis. tITP is widespread as a very useful method for inline sample preconcentration.

Electric field gradient focusing

Concepts of EFGF

Electric field gradient focusing (EFGF) methods use separation systems in which an electric field gradient is induced. Focusing occurs when analytes at opposite sides of the gradient migrate in opposite directions to a point where they have zero velocity on the gradient.

In some cases, the gradient may move as a whole, for example by electromigration. Therefore, it is more precise to define the analyte velocities relative to the gradient velocity $\mathbf{v}_{\text{gradient}}$. The analyte focusing locations are the points on the gradient where the velocities of the analytes are equal to the velocity of the gradient ($v_i = v_{gradient}$). The change of sign in ion velocity should then be regarded as being relative to the gradient velocity.

Moreover, we take the flow velocity as a frame of reference. The velocities of the ions and of the gradient therefore must be corrected for flow velocity. In many counterflow gradient focusing methods, the gradient has a constant position in the channel structure. In these situations, we take the gradient velocity as minus the flow velocity ($v_{gradient} - v_{flow} = 0$). These considerations will make a direct comparison of EFGF and ITP more straightforward.

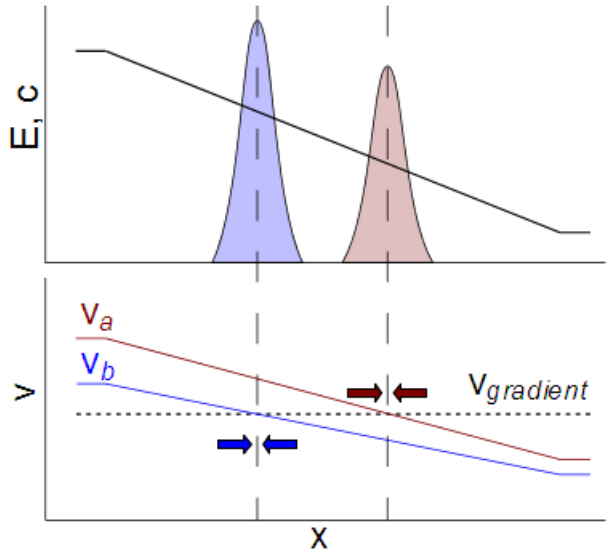

Figure 2. Common principle of EFGF methods. In the graphs, the electric field profile (E) is sketched, as well as the concentration (c) and velocity (v) profiles for two analytes. Analytes focus at the point where the electrophoretic velocity is equal to the gradient velocity, these points are indicated by vertical dashed lines.

Figure 2 shows a schematic electric field gradient as might be used in EFGF, as well as the resulting velocities of ions *a* and *b* with ionic mobilities $\mu_a > \mu_b$

versus the gradient velocity. The figure shows how the ions obtain different focusing positions dependent on their ionic mobility.

Analytes may have too low or too high ionic mobility to be focused on a gradient. These analytes are not trapped.

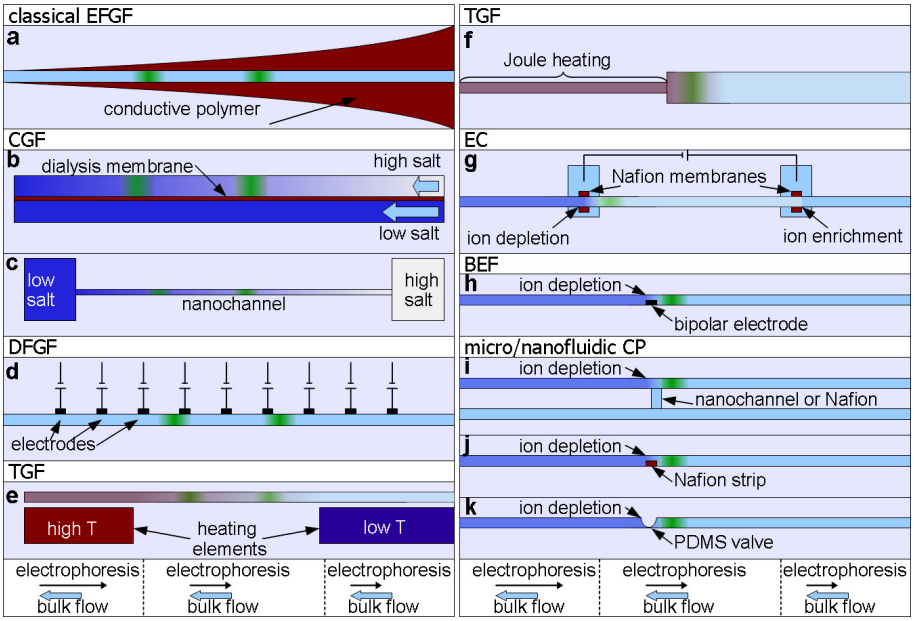

Figure 3. Overview of several EFGF methods and variants thereof. These methods are discussed in detail in the text. The green bands indicate analyte focusing positions, where electrophoretic velocity is equal to bulk flow velocity

We will proceed to discuss the numerous EFGF methods that have been published to date. EFGF methods are often compared to isoelectric focusing (IEF), which is one of the oldest and most well-known electrokinetic focusing methods. In IEF, amphoteric compounds are allowed to migrate through a pH gradient, resulting in adjustment of the net charge of the compounds, until they reach their isoelectric point (pI). IEF is particularly powerful for proteins, though precipitation often can be a limitation. In contrast to the EFGF methods discussed here, compounds obtain zero net mobility when focused

by IEF. Because this results in different physics, we do not regard IEF and related techniques like the dynamic pH junction method[53] as forms of EFGF, and therefore these methods will not be further considered in this review. The most important EFGF approaches are summarized in figure 3. These EFGF methods will be discussed in detail in the following sections.

Classical EFGF

Electrical field gradient focusing (EFGF) was introduced by Koegler and Ivory[54, 55], who focused and separated proteins in a dialysis tubing which was placed in a converging channel. The converging channel shaped the electric field while the dialysis tubing helped to maintain a pressure-driven counterflow with uniform velocity. We will call this and similar methods "classical EFGF". For example, Humble et al used a miniaturized device in which they molded a linear channel into a converging area filled with conductive polymer (figure 3a), yielding an electric field gradient upon voltage application. With their device, they achieved separation of up to 5 proteins as well as 10 000 fold preconcentration.[8] Liu et al. also performed focusing and separation of protein mixtures and showed selective elution of protein peaks by increasing counterflow rate.[56] Changing the voltage drop also can result in selective elution, as was demonstrated by Wang et al.[57] Petsev et al. used a chip design in which the separation channel had several side channels in order to introduce step changes in the electric field[58].

CGF

In conductivity gradient focusing (CGF), an electric field gradient is formed by creating a gradient in electrolyte conductivity. CGF was introduced by

Greenlee and Ivory[59] who used a setup containing a separation channel and a purge channel which were separated by a dialysis membrane. The separation channel had a high-salt inlet; the high-salt electrolyte was gradually diluted by dialysis through the low-salt purge channel (figure 3b). They were able to focus and separate a binary protein mixture.

Inglis et al used a conductivity gradient inside a nanochannel which connected a high salt and a low salt reservoir (figure 3c). An electro-osmotic flow provided the necessary counterflow. Two proteins were separated and 1000-fold preconcentration was achieved.[60]

DFGF

Dynamic field gradient focusing (DFGF) was introduced by Huang and Ivory.[61] They used an array of individually controllable electrodes which were placed inside the separation channel for detailed control of the electric field gradient (figure 3d). Tracey et al. described a preparative scale DFGF instrument prototype.[62, 63] Burke et al. used DFGF for simultaneous separation of negatively and positively charged proteins. Focused peaks could be positioned, the authors even demonstrated that the positions of focused proteins could be swapped by locally changing the electric field gradient during the experiment.[64]

TGF

Temperature gradient focusing (TGF) was introduced by Ross and Locascio[9], who used a device with external heating blocks (figure 3e). A Tris/borate buffer was used because the conductivity of this buffer depends relatively strongly on temperature (more strongly than analyte ionic mobilities, which

are also affected by temperature). This results in an electric field gradient on which analytes could be focused. A wide range of compounds could be focused, including labeled amino acids, proteins, DNA and polystyrene particles. 10 000 fold preconcentration was achieved. Ross and Locascio also showed that Joule heating in a narrow channel section can be used for TGF (figure 3f), an effect which was studied more extensively in other publications[65-67]. Another interesting method to introduce a temperature gradient is optothermal heating. Akbari et al. used a digital projector as a light source and heater which could be moved in order to position a focused fluorescein zone.[68]

Balss et al. used TGF to perform two different DNA hybridization assays. In a first assay, a DNA target was focused and peptide nucleic acids (PNA) were introduced in the bulk flow, resulting in PNA-DNA hybridization. In a second assay, bulk flow was varied to move focused PNA-DNA duplexes through the temperature gradient in order to measure their melting temperature[69]. To overcome the limitation that only a few components can be simultaneously focused and separated on a temperature gradient, Hoebel et al. introduced scanning TGF in which the bulk flow is varied to obtain sequential focusing and elution of a larger number of compounds[70].

EC

Electrocapture (EC) devices use a capillary or tubing containing two Nafion junctions. The Nafion junctions are connected to reservoirs which contain a high and a low voltage electrode. A pressure-driven flow was applied to the capillary. Applying a voltage leads to concentration polarization across the Nafion junctions, resulting in ion enrichment at the upstream junction and

ion depletion at the downstream junction. On the resulting conductivity gradients analytes can be focused (figure 3g). Adjusting the flow rate leads to selective release of compounds. EC has been reviewed by Shariatgorji et al.[71] The technique has mainly been applied to proteins, peptides and DNA and has been used for preconcentration, separation, salt and detergent removal, buffer replacement and inline reactions. Importantly, EC could be coupled to mass spectrometry (MS)[72, 73]. To our knowledge, no other EFGF technique has been successfully hyphenated with MS yet. To date, EC also appears to be the only commercialized EFGF method[74].

BEF

Bipolar electrode focusing (BEF) was introduced by Dhopeshkarwar et al.[75], who used a simple linear channel containing an electrically floating bipolar electrode. When a voltage was applied over the channel, local ion depletion occurred at the bipolar electrode location. On the resulting conductivity gradient analytes could be focused (figure 3h). The ion depletion zone appears to be caused by electrode reactions[76]. Interestingly, if the bipolar electrode was connecting two parallel microchannels, a faradaic form of concentration polarization occurred, with ion enrichment in the cathodic channel[6]. This configuration is very similar to the H-shaped concentration polarization devices discussed below. Up to 500 000 fold concentration enrichment was reported with this device. In a similar dual channel configuration, cations and anions could be separated and enriched simultaneously[77].

Concentration polarization; micro/nanofluidic CP devices

Concentration polarization (CP) is a well-known phenomenon from membrane technology, which has gained considerable attention in the last 10 years from researchers of micro- and nanofluidic separations. Since 2005, when Wang et al.[4] developed an elegant implementation of the principle in a micro/nanofluidic device, chip-based CP devices have attracted much attention. A detailed review of CP theory has been published recently[78], simultaneously with a review of micro/nanofluidic CP devices[79].

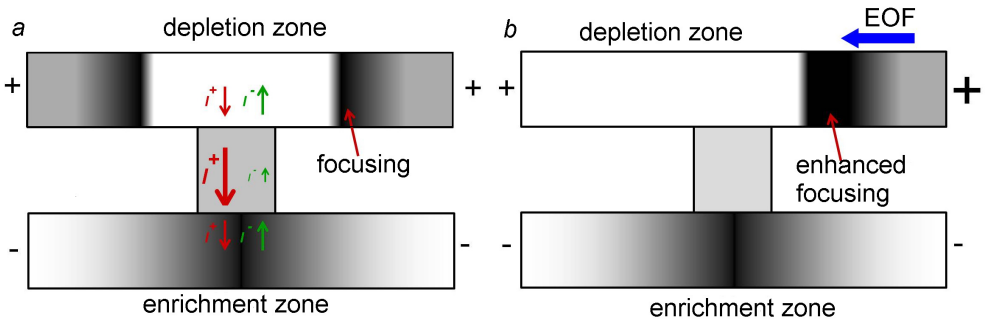

Figure 4. Phenomena in concentration polarization devices. a) Formation of depletion and enrichment zones due the imbalance of cation versus anion flux inside the nanochannel. b) Inducing a tangential EOF results in analyte trapping at the upstream border of the depletion zone.

CP is a phenomenon that can occur across nanopores and nanochannels. Upon applying a voltage across a nanochannel, ions (both cations and anions) accumulate at one entrance of the nanopore while being depleted at the opposite entrance. This effect can be ascribed to the surface charge of the material of which the nanochannel is made. Often used materials like glass, silicon and PDMS have a negative surface charge, particularily at high pH's, due to deprotonation of silanol groups (equilibrium of SiOH and SiO^-).

Because in a nanochannel the walls are very close to one another, surface charges can become dominant, resulting in coion exclusion and counterion enrichment inside the nanochannel (figure 4). While electrical current through a microchannel is carried equally (in a sense) by anions and cations, it must be carried mostly by cations inside a nanochannel with a negative surface charge. In other words, cation flux inside the nanochannel is higher than in the adjacent microchannel or reservoir; while anion flux is lower. A simple summation of ion fluxes reveals that both cations and anions are enriched at the cathodic side of the nanochannel and depleted at the anodic side (in the case of a negative surface charge). Thus, enrichment and depletion zones are formed (figure 4a)[80, 81].

In the aforementioned publication of Wang et al[4], an H-shaped channel geometry was used, comprising a nanochannel which connected two parallel microchannels. CP across the nanochannel induced depletion zone formation in one of the microchannels. A tangential electric field induced an electroosmotic flow (EOF) through this microchannel, carrying charged analytes. Due to the conductivity difference at the depletion zone border, the analytes can be trapped very efficiently (figures 3i, 4b). Over 10 000 000 concentration factors were reported[4]. With a similar device, Kim et al. reported similar concentration factors for protein preconcentration.[5] Though this latter author casted some doubt on this result because it would require extraordinarily high flow velocities, it is evident that very efficient preconcentration could be achieved. Wang et al. and Kim et al. also demonstrated a zone electrophoresis separation after preconcentration. Many methods have been published to produce similar devices[79]. These devices have been used for enzyme assays[82-84], immunoassays[85-88], inline labeling[89] and

desalination[90]. Moreover, massive parallelization of the device also has been achieved[88, 91]. Interestingly, the ion depletion effect also can be induced in a single channel by placing a Nafion patch. Electric field lines going through the Nafion induce depletion zone formation, providing a focusing gradient (figure 3k)[7, 92]. Alternatively, elastomeric valves in PDMS devices also can be employed, in "closed" state, leaving a nanogap between the valve membrane and the channel wall, which can be used to induce CP and preconcentration effects (figure 3j, see also chapter 3)[93, 94].

ITP and EFGF intertwined

EFGF processes in ITP

In ITP, focusing occurs in conjuction to gradient effects, supporting the view that ITP is a form of EFGF. Diffusion effects create overlap between adjacent zones, resulting in an electric field gradient on which analytes with intermediate mobility will be focused.

With regard to focusing effects, many authors refer to ITP as a stacking method. However, as a concentration mechanism, stacking should be discerned from focusing: during focusing ion velocities change of sign, while in stacking ion velocities change in magnitude but not of sign. In ITP, stacking indeed plays a role, but focusing is the principal mechanism for concentration and separation of analytes.

Figure 5 shows a scheme of a conventional ITP separation in which one analyte has reached plateau concentration while three other analytes are in peak mode. The corresponding electric field is also shown. Clearly, two gradients are present: one between the TE and the analyte plateau, and one

between the analyte plateau and the LE. The peak mode analytes are focused on these gradients.

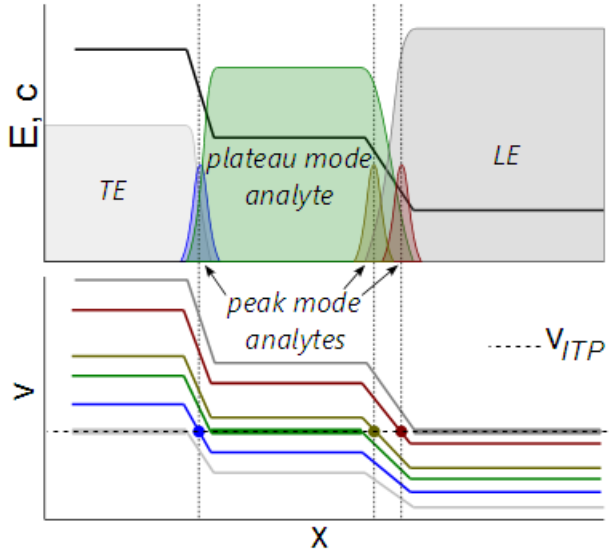

Figure 5. Profiles of electric field (E), ion concentrations (c) and ion velocity profiles (v) in an ITP separation containing a LE, a TE, a plateau mode analyte and three peak mode analytes. Focusing occurs at locations where analyte velocity is equal to the ITP velocity. Focusing locations of peak mode analytes are indicated by vertical dotted lines.

When comparing figure 2 and figure 5 the similarities between EFGF and ITP become evident. In both situations, ions are focused at the points where their velocities are equal to the gradient velocity, the locations of these points differing depending on the ionic mobility. The most significant difference between the figures is that one of the analytes in figure 5 reaches a plateau. Plateau concentration ions have a line instead of a single point on which the ion velocity is equal to the isotachophoretic velocity v_{ITP} (which is the equivalent of $v_{gradient}$). For peak mode ions the only difference is that multiple gradients are present.

The two peaks in figure 5, which are situated between the analyte plateau and the LE are focused at slightly different positions. Due to the self-correcting mechanism of ITP, the gradients on which peak mode ions are focused are often very steep. Multiple ions on a single gradient therefore usually can not be resolved as individual peaks. However, Khurana et al. used the slow reaction kinetics of carbonate ions with an amine-containing TE to create a shallow gradient between the TE and the LE on which multiple DNA molecules could be separated in resolved peaks[95].

ITP processes in EFGF methods

In an EFGF experiment, analyte ions are focused on a fixed position on a gradient. This implies that upon completion of the focusing process all focused analytes have the same velocity. In other words, gradient focusing results in something to which the term iso-tacho-phoresis may be applied very literally. For analytes focused on a gradient the isotachophoretic condition holds. We have seen that from this condition a number of notable characteristics can be derived: each co-ion will form a pure, sharply defined zone with a plateau concentration and with an electric field which is adjusted to the ionic mobility of the co-ion concerned. Therefore it can be predicted that in EFGF analytes will form adjacent plateau-shaped zones similar to conventional ITP. Just as in conventional ITP, such plateau zones will only form if sufficient analyte is present. If analytes are present in low quantities only, EFGF will be similar to peak mode ITP.

A significant difference between current-day EFGF and ITP methods is that EFGF does not require a discontinuous electrolyte system with a LE and a TE. Using a LE and a TE is the most common method to impose the

isotachophoretic condition on a separation. There is however no reason to assume that this is the only method. Gradient focusing also has an isotachophoretic outcome, simply because immobilization on a gradient results in equal velocities for the focused analytes. Moreover, several crucial ITP parameters do not depend on TE parameters. The dependence of plateau concentrations on LE (and not TE) concentration has already been pointed out. Additionally, analyte zone speed and width are (at least in peak mode ITP) independent of TE conductivity.[48]

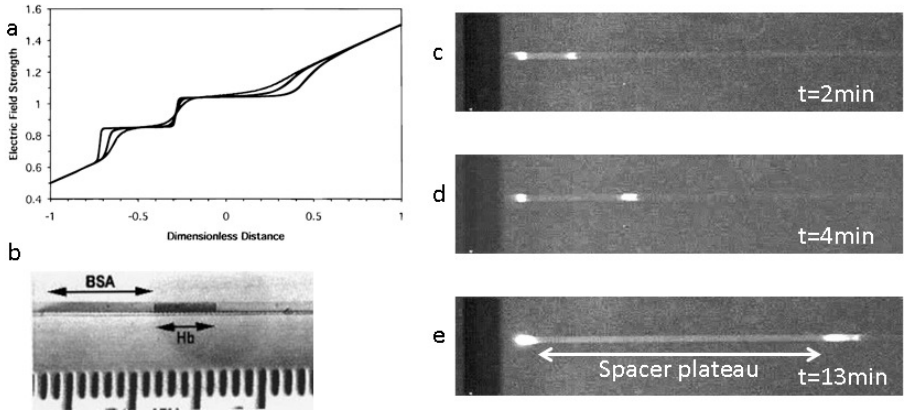

Figure 6. Indications of ITP processes in several EFGF methods: a) Koegler simulated the electric field yielding a stair-like pattern that is typical for ITP (reproduced with permission from ref 55); b) Greenlee found sharply defined contiguous analyte plateau sones in CGF (reproduced with permission from ref 59); c-e) In BEF, Laws found a separation of two focused zones by a continuously growing zone, indicating the insertion of a spacer (reproduced with permission from ref 99).

Important hallmarks of ITP have been described already in early papers on EFGF methods. Koegler and Ivory[55] performed modeling of classical EFGF and showed that the electric field gradient evolved into a stair-like profile if sufficiently high concentrations of two model analytes were provided (figure 6a). A stair-like electric field gradient is very characteristic for ITP. However,

in their analysis the corresponding analyte zones did not clearly have a plateau shape, though clearly deviating from a Gaussian profile. Nevertheless, in the experimental section of the same paper, an absorbance trace of separated myoglobins shows an analyte zone with a plateau-like shape.

In conductivity gradient focusing, Greenlee and Ivory observed wide contiguous bands of BSA and hemoglobin. The border between these bands was very sharply defined and the concentration throughout the bands appeared to be constant (figure 6b). The authors noted that such bands are characteristic for ITP, but viewed the isotachophoretic effect as undesired[59].

Lin et al[96] studied finite sample effects in TGF (i.e. situations in which sample concentration is large enough to affect the electric field distribution) using a model based on a generalized Kohlrausch regulation function. Experimental results were used to verify some of their observations. In TGF, plateau-shapes are not expected for concentration profiles, since the temperature gradient significantly affects analyte mobility. However, the velocity profiles in the simulations of Lin et al. showed a plateau-shaped zone which broadened over time. The study of Lin et al. did not include multiple analyte ions, which we predict to reveal multiple ITP-like zones.

For EC, Astorga-Wells et al.[97] compared flow velocities and measurements of local electric fields. If the background electrolyte is migrating with equal, but opposite velocity with respect to the flow velocity, the ratio $\mathbf{v}_{flow}/\mathbf{E}$ should be equal to the ionic mobility of the background electrolyte ions (see also eq 2). At low flow velocities, this was indeed the case for several background electrolytes, which points at stable zones of immobilized background electrolyte. Moreover, the upstream local electric field was independent of the externally applied voltage (using equal flow velocities), which is evidence of

local electric field adjustment to the isotachophoretic condition: ions in plateau mode must have a uniform value of the ratio $\mathbf{v}_{flow}/\mathbf{E}$. At higher flow velocities, the concentration polarization effect broke down and the focusing condition was no longer present. In the same research, separation of analytes into adjacent zones was observed, although it was not clear whether these zones were peaks or plateaus. The authors explained their findings as being consistent with ITP.

In BEF, Hlushkou et al.[98] observed both in experiments and simulations that a focusing analyte (bodipy disulfonate) reached a plateau concentration independent of the starting concentration. This plateau concentration was about five times lower than the electrolyte concentration (1 mmol/L TrisHCL). Simulated profiles of the electric field distribution revealed a growing plateau, which extended the electric field gradient. Although the authors do not mention ITP effects as a possible explanation, we do think their results are consistent with ITP. In another paper on BEF, Laws et al.[99] used up to three fluorescent analytes, which they were able to separate. Although some of these separations appeared to occur in peak mode, one of the video's in the supplementary information of that paper clearly showed a rapidly broadening weakly fluorescent zone, which spaced some other analytes apart (figure 6 c-e). The length of this zone (>5 mm) stretched well beyond the predicted range of the electrode-induced electric field gradient. The fluorescence intensity in this zone appeared to be approximately constant. The authors did not comment on this zone in their paper, but we strongly suspect that it has an isotachophoretic nature. Finally, in a recent publication describing BEF focusing of the cationic species $[Ru(bpy)_3]^{2+}$, the formation of a plateau-shaped analyte zone was also observed[100].

dzITP

The clearest case of an ITP separation induced by EFGF is perhaps depletion zone isotachophoresis (dzITP). dzITP was recently developed in our lab using conventional H-shaped micro/nanofluidic CP devices (figure 7a)[101]. At the upstream border of the depletion zone, analytes were focused and, if present in sufficient concentrations, plateau zones were readily formed (figure 7b). Discrete and continuous injections were performed for up to four fluorescent analytes and were separated in ITP zones. Using a non-fluorescent spacer, it was possible to elute a focused 6-carboxyfluorescein zone towards the upstream reservoir, while keeping fluorescein focused at a stable position at the depletion zone border (figure 7c). Moreover, positioning of the dzITP zones was possible by controlling the length of the upstream part of the depletion zone by means of voltage actuation. In a second paper on dzITP, we demonstrated the tunability of the ionic mobility window[102]. Focused compounds could be released along the depletion zone in the downstream part of the channel. Similar to a valve that can be opened to several extends, the flux of released compound could be controlled. This was used for both pulsed and continuous release. In continuous mode, a balance of fluxes of released and supplied compound established filter action. A marker compound was partially released, defining the ionic mobility cut-off. Undesired compounds are coreleased while compounds in the desired ionic mobility window are trapped behind the marker compound zone. This principle was applied to selectively enrich 6-carboxyfluorescein over lower-mobility fluorescein despite having a 250x lower starting concentration; to achieve this, acetate was used as a non-fluorescent spacer to establish the ionic mobility cut-off between fluorescein and 6-carboxyfluorescein (figure

7d). Additionally, for dilute raw urine fluorescein was used as a marker compound while simultaneously acting as an underspeeding tracer for indirect detection.

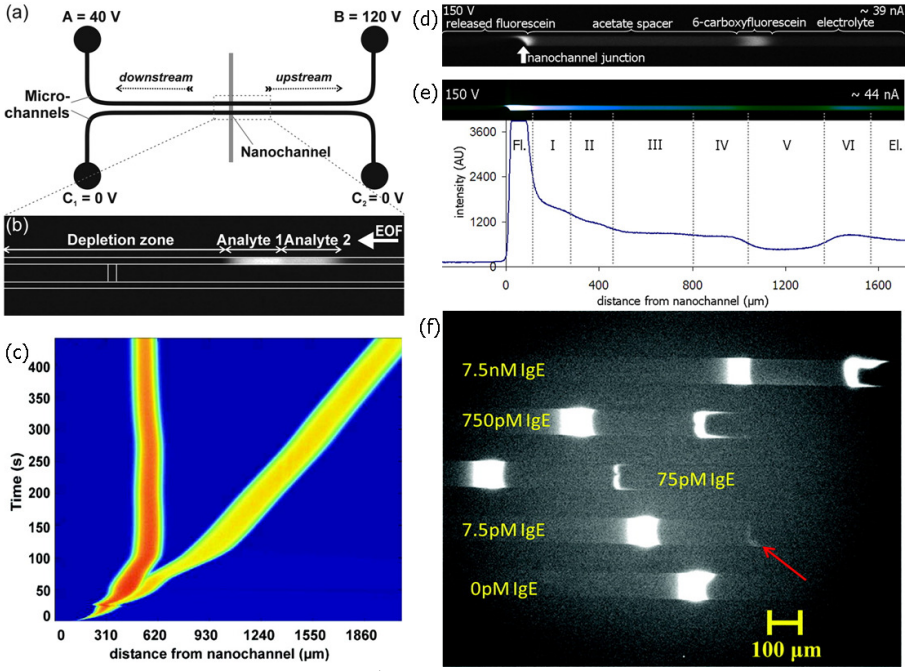

Figure 7. Functionality of dzITP. a) Schematic representation of a H-shaped concentration polarization device as used for depletion zone isotachophoresis. b) dzITP-separated zones at the border of a depletion zone. c) Spatiotemporal plot of a dzITP separation using a discrete injection of fluorescein and 6-carboxyfluorescein and a continuous injection of acetate. The acetate acts as a non-fluorescent spacer, eluting focused 6-carboxyfluorescein while fluorescein remains trapped at the border of the depletion zone. Images a-c reproduced with permission from ref. 101. d) selective enrichment of 6-carboxyfluorescein over fluorescein by ionic mobility filtering. e) Selective trapping and indirect detection of urine compounds using fluorescein as a marker. Fl.: fluorescein. El.:electrolyte. The Roman numerals I-VI indicate putative analyte zones. Images d and e reproduced with permission from ref. 102. f) Fluorescent aptamer assay for detection of several concentrations of IgE. The left fluorescent band arises from unbound aptamer, the band on the right arises from IgE-bound aptamer. The bands are spaced by non-fluorescent BSA protein. Image reproduced with permission from ref. 86.

This way, several urine constituents within a specific ionic mobility window were efficiently enriched and separated into distinct zones (figure 7e). Cheow et al[86] used dzITP in ultrasensitive IgE and HIV-1 RT assays, using fluorescent aptamers for detection. BSA was used as a non-fluorescent spacer between bound and unbound aptamer, improving detection (figure 7f).

Implications and perspectives

Unification of ITP and EFGF

In this review we have presented an argument for the unification of the concepts of ITP and EFGF. The bottomline of this argument is that ITP and EFGF are both founded on the isotachophoretic principle: all focused ions migrate with the same velocity in a completed separation. From the isotachophoretic principle many hallmarks of ITP can be derived, all of which have been observed in simulations and/or experimental research of EFGF methods. This includes the existence of analyte plateau concentrations independent of analyte starting concentrations but dependent on leading electrolyte concentration, adjustment of local electric field to the isotachophoretic condition, the formation of contiguous analyte bands, and the observation of plateaus in electric field and analyte velocity. Moreover, typical ITP tricks like the use of spacers and tracers can be applied to EFGF methods.

A possible counterargument is that EFGF methods generally do not use a discontinuous electrolyte system, comprising a LE and a TE in conventional ITP. However, the use of a LE/TE system should be regarded as one of the many ways in which the isotachophoretic condition can be imposed on a separation. Focusing gradients can be a fully-fledged alternative to a TE zone.

To underscore the role of ITP processes in EFGF, it will be useful to speak of peak mode and plateau mode EFGF, similar to peak mode and plateau mode ITP. Plateaus give a maximum to preconcentration, lead to alterations of the gradient profile, but also extend the separation beyond the original range of the gradient (figure 8) and give the possibility to apply many ITP tricks.

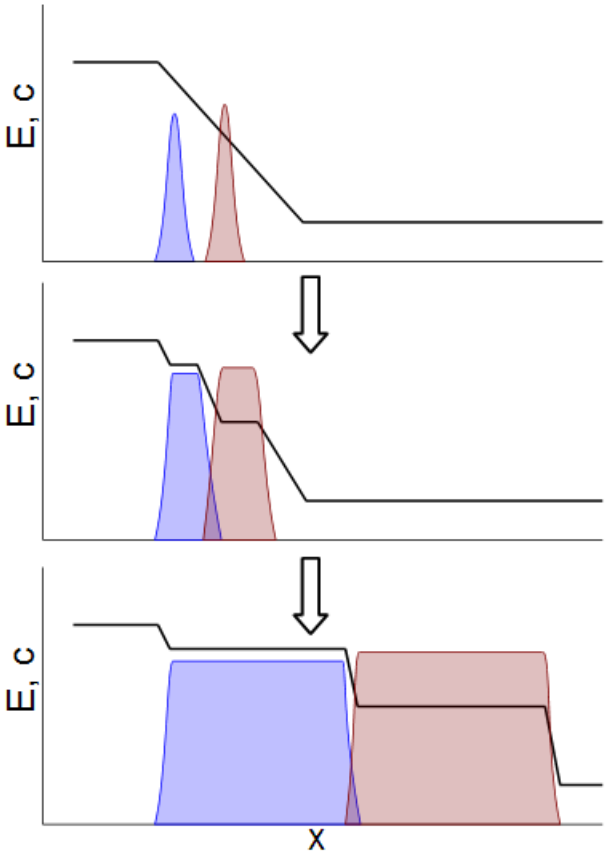

Figure 8. Transition from peak mode to plateau mode in EFGF. In peak mode (above), the electric field gradient is hardly affected by the focusing analytes. During the transition (middle), plateaus will form in the electric field gradient. After prolonged focusing in plateau mode, the analyte plateaus can grow far beyond the range of the original gradient (below).

Advantages and disadvantages of EFGF

EFGF techniques have several crucial advantages over conventional ITP, providing extra versatility which may make an EFGF technique a method of first choice. First, EFGF methods generally are single-electrolyte methods (CGF is an exception). This makes injection procedures more straightforward,

saves preparation and consumption of electrolyte solutions and will make EFGF more accessible to untrained personnel.

Second, EFGF can be induced at predefined and stable positions. This is also possible in ITP, but that requires special counterflow protocols. In DFGF and BPE, the focusing locations are simply determined by the placement of electrode(s), in TGF by the placement of heater elements, in EC and dzITP by the location of the nanochannel or nanoporous membrane, etc. Monitoring of the focusing and separation process is more straightforward with these methods.

Third, in many EFGF methods zone positioning is possible. This can be done by varying the counterflow, resulting in a shift of focusing positions. In TGF positioning also can be done by changing the location of the heater element, in DFGF by changing the voltage differences between the individual electrodes, and in dzITP by varying the position of the depletion zone border. Zone positioning allows repeated and on-demand detection, specific reactions and interactions with zones containing certain coatings and gels, and manipulations with local physical perturbations such as a magnetic field.

Fourth, in several EFGF methods, including classical EFGF, DFGF, CGF and TGF, shallow gradients can be created, which is useful for resolving individual peaks with close mobilities. In conventional ITP this is often problematic.

Finally, in EFGF methods the ionic mobility window can be tuned during the experiment, for example by changing the counterflow velocity, or by varying the differences in electric field, or (as in dzITP filtering) by adjusting the balance between supply and release fluxes.

This provides enormous versatility in the selectivity of EFGF methods, which can be used for enrichment and purification strategies, as well as for

sequential trapping and analysis of different classes of compounds based on ionic mobilities.

EFGF methods have also a few disadvantages compared to conventional ITP. Perhaps the most important disadvantage is that EFGF methods require dedicated instrumentation, while conventional ITP can be performed in a simple CE capillary. Conventional ITP is compatible with commercial CE apparatuses while for EFGF methods hardly any commercial equipment exists (with the exception of EC[74]). With regard to miniaturization, on-chip ITP does not require the special components needed for EFGF methods like membranes, electrodes, heating elements or nanochannels. A second disadvantage, which affects only a limited range of applications, is that trailing-side injections are often difficult or even not possible in EFGF methods. In counterflow methods, the flow can strongly oppose trailing-side injections. Moreover, analyte velocity often only locally changes of sign. Consequently, trailing-side injected analytes are not transported towards the focusing region. Trailing-side injections may be crucial for some assays based on conventional ITP, for example when extracting high-mobility nucleic acids from low-mobility protein inhibitors.[103] Such assays might have poor feasibility with many EFGF-induced ITP methods.

Synergism of ITP in EFGF

The insight that EFGF methods have ITP nature leads to the realization of several important ITP phenomena in EFGF. An important aspect is that ITP can form zones that are pure with respect to co-ions. The insight that such zones also can be formed by EFGF may be useful for purification applications. A powerful ITP trick is the use of spacers. The baseline separation that may be

obtained by the use of a spacer is not only very useful for detection, but also for (bio)chemical assays. For example, undesired reactions may be prevented. Additionally, a reaction may be monitored by quantifying the amount of reaction product that is transferred across a spacer zone. Indirect detection by non-focusing tracers, such as the counterspeeder and underspeeder concept originally developed for ITP, is also applicable to EFGF. Another important lesson from ITP is that zones can grow indefinitely if sufficient compound is present. Similarly, in EFGF zones may grow beyond the range of the original gradient (figure 8). So if in EFGF plateau zones are allowed, peak capacity is not limited by the range of the gradient, but rather by the length of the separation channel upstream from the gradient.

Table 1 lists a number of features that are demonstrated or predicted in ITP and EFGF methods. Most demonstrated features have been discussed in the previous sections, and have been referenced if not so. The predicted features have been extrapolated from observations of similar features in other EFGF methods and may require adjustments of existing methods. In some cases a feature might not be available due to intrinsic limitations of a method. From table 1, a number of important observations can be made. First, all features demonstrated in conventional ITP have also been demonstrated in one or more EFGF methods. CP devices (including dzITP) stand out in this regard. Second, as discussed in the previous section, EFGF methods have several features not being available with conventional ITP, providing important extra functionality and simplicity of use. Third, once the predicted features are realized, these features might be combined at will, making each EFGF method a very versatile toolbox for bioanalysis.

Table 1 Predicted and demonstrated features of ITP/EFGF methods

Feature	(transient) ITP	Classical EFGF	CGF	DFGF	TGF	BEF	EC	CP devices & dzITP
Analyte plateau zones	**d**	**d**	**d**	p	p	**d**	p	**d**
>10 000 fold preconcentration	**d**	**d**	p	p	**d**	**d**	p	**d**
Separation of proteins and peptides	**d**	**d**	**d**	**d**	**d**	p	**d**	**d**
Separation of nucleic acids	**d**	p	p	p	**d**	p	**d**	p
Separation of small molecules/ions	**d**	**d**	p	p	**d**	**d**	p	**d**
Dynamic control of analyte zone position		p	p	**d**	**d**	**d**[103]		**d**
Dynamic control of ionic mobility window		**d**	p	p	**d**	**d**[104]	**d**	**d**
Use of spacer compounds	**d**	p	p	p	p	p	p	**d**
Indirect analyte detection using tracers	**d**	p	p	p	p	p	p	**d**
Single electrolyte		**d**		**d**	**d**	**d**	**d**	**d**
Desalting	**d**[105]		p			p	**d**	**d**
Enzyme assays	**d**[106]	p	p	p	p	p	**d**[107]	**d**
Immunoassays	**d**[108]	p	p	p	p	p	p	**d**
Nucleic acid hybridization assays	**d**	p	p	p	**d**	p	p	p
Hyphenation with CE	**d**	p	p	p	p	p	**d**[109]	**d**
Hyphenation with MS	**d**	p	p	p	p	p	**d**	p

d = demonstrated, p = predicted

Opportunities and outlook

With so many potential advantages for sensitivity and selectivity, ITP/EFGF methods will have many breakthrough applications in diverse fields of biology, including -omics studies, biomarker discovery, drug discovery and diagnostics. So far, all methods described above have been implemented either as a microfluidic setup, a capillary setup, or preparative scale setup. We expect particular benefit from the microfluidic and capillary setups in distinctive application fields.

For capillary ITP/EFGF setups we foresee highest impact in hyphenated settings. The use of transient ITP to enhance CE separations has already been proven a powerful technique. Increased usability is expected as the LE/TE buffer system is replaced with a single electrolyte system, simplifying sample preparation and injection procedures. In addition, the intrinsic concentration and clean-up capabilities of such a system may add to the reproducibility and sensitivity of CE separations. Another promising application will be direct hyphenation with mass spectrometry (MS). Electrocapture and concentration polarisation devices have shown powerful performance in desalting of samples, an operation that is highly important to prevent ion suppression in electron-spray mass spectrometry. Furthermore, dzITP has shown that focused analyte bands can be selectively released, enabling transport to the electrospray emitter on a band-by-band basis. This will also enhance sensitivity of MS-based detection. The clearest demonstration of this potential so far has been demonstrated in electrocapture[72]. EFGF methods will raise the quality of ITP separations and become an attractive complement or even an alternative for current day CE-MS, HPLC-MS and direct infusion MS techniques.

For microfluidic setups, the biggest opportunities lie in the field of molecular interaction assays. For such type of assays, the fact that one can trap molecular species in solution reduces surface interactions that are a typical disturbance in solid-phase immobilized assays. The fact that molecular compounds of lower mobility or opposite charge can be flushed through focused analyte zones dramatically increases binding and interaction efficiencies. Similar opportunities exist for multiple reagents that are concentrated in overlapping peak mode zones. Quantification through

measurement of zone growth enables real-time determination of binding constants and enzyme activity. A promising example is the aptamer dzITP assay presented by Cheow et al.[86] When adding functionality like selective ionic mobility filtering and the use of spacers and tracers, a molecular interaction platform of unprecedented versatility is obtained. We envision many impactful biochemical assays, including protein-protein and protein/nucleic acid interaction assays for determining binding constants; enzyme activity assays, amongst which protein kinase-inhibitor assays are important as many kinases play a significant role in cancer and other diseases; immunoassays; metabolite-protein interaction platforms for drug discovery purposes; and nucleic acid hybridization assays. These assays, being made sensitive and specific, do not necessarily require complicated instrumention like MS or NMR, but will become available as stand-alone benchtop instruments for rapid diagnostics suitable for clinical settings. By integrating microelectronics and miniaturized detection technology, ITP/EFGF methods will be available as hand-held analyzers[111] that may be used for water and food quality monitoring, homeland security and point-of-care diagnostics.

Conclusion

A large number of EFGF and ITP techniques have been developed to-date and a wide range of applications and functionality have been demonstrated. In this review we have presented arguments and strong evidence from literature for the unification of both techniques, implying that EFGF and ITP functionality might be integrated on a single platform. This combined toolbox includes amongst others ultra-efficient and selective preconcentration, separation, tunable analyte focusing windows, requirement of a single

electrolyte only, and the ability to desalt and clean-up samples. Among the most promising applications are hyphenation with CE and MS for -omics studies and biomarker discovery, as well as a wide range of molecular interaction assays for drug screening and clinical diagnostics.

References

1. B. Jung, R. Bharadwaj and J. G. Santiago, Analytical Chemistry **78** (7), 2319-2327 (2006).
2. D. Bottenus, T. Z. Jubery, Y. Ouyang, W.-J. Dong, P. Dutta and C. F. Ivory, Lab on a Chip **11** (5), 890-898 (2011).
3. J. Wang, Y. Zhang, M. R. Mohamadi, N. Kaji, M. Tokeshi and Y. Baba, Electrophoresis **30** (18), 3250-3256 (2009).
4. Y.-C. Wang, A. L. Stevens and J. Han, Analytical Chemistry **77** (14), 4293-4299 (2005).
5. S. M. Kim, M. A. Burns and E. F. Hasselbrink, Analytical Chemistry **78** (14), 4779-4785 (2006).
6. R. K. Anand, E. Sheridan, K. N. Knust and R. M. Crooks, Analytical Chemistry **83** (6), 2351-2358 (2011).
7. M. Kim, M. Jia and T. Kim, Analyst (2013).
8. P. H. Humble, R. T. Kelly, A. T. Woolley, H. D. Tolley and M. L. Lee, Analytical Chemistry **76** (19), 5641-5648 (2004).
9. D. Ross and L. E. Locascio, Analytical Chemistry **74** (11), 2556-2564 (2002).
10. Z. K. Shihabi, Journal of Chromatography A **902** (1), 107-117 (2000).
11. J. L. Beckers and P. Boček, Electrophoresis **21** (14), 2747-2767 (2000).
12. D. M. Osbourn, D. J. Weiss and C. E. Lunte, Electrophoresis **21** (14), 2768-2779 (2000).
13. M. Urbánek, L. Křivánková and P. Boček, Electrophoresis **24** (3), 466-485 (2003).
14. R.-L. Chien, Electrophoresis **24** (3), 486-497 (2003).
15. C.-H. Lin and T. Kaneta, Electrophoresis **25** (23-24), 4058-4073 (2004).
16. M. C. Breadmore, Electrophoresis **28** (1-2), 254-281 (2007).
17. Z. Malá, A. Šlampová, P. Gebauer and P. Boček, Electrophoresis **30** (1), 215-229 (2008).
18. S. L. Simpson Jr, J. P. Quirino and S. Terabe, Journal of Chromatography A **1184** (1–2), 504-541 (2008).

19. M. C. Breadmore, J. R. E. Thabano, M. Dawod, A. A. Kazarian, J. P. Quirino and R. M. Guijt, Electrophoresis **30** (1), 230-248 (2009).
20. M. C. Breadmore, M. Dawod and J. P. Quirino, Electrophoresis **32** (1), 127-148 (2011).
21. L. Kartsova and E. Bessonova, Journal of Analytical Chemistry **64** (4), 326-337 (2009).
22. Z. Malá, P. Gebauer and P. Boček, Electrophoresis **32** (1), 116-126 (2011).
23. B. C. Giordano, D. S. Burgi, S. J. Hart and A. Terray, Analytica chimica acta (2012).
24. Y. Chen, W. Lü, X. Chen and M. Teng, Central European Journal of Chemistry, 1-28 (2012).
25. A. Šlampová, Z. Malá, P. Pantůčková, P. Gebauer and P. Boček, Electrophoresis (2012).
26. C.-C. Lin, J.-L. Hsu and G.-B. Lee, Microfluidics and Nanofluidics **10** (3), 481-511 (2011).
27. K. Sueyoshi, F. Kitagawa and K. Otsuka, Journal of separation science **31** (14), 2650-2666 (2008).
28. M. C. Breadmore, A. I. Shallan, H. R. Rabanes, D. Gstoettenmayr, A. S. Abdul Keyon, A. Gaspar, M. Dawod and J. P. Quirino, Electrophoresis **34** (1), 29-54 (2013).
29. C. J. Holloway and I. Trautschold, Fresenius' Journal of Analytical Chemistry **311** (2), 81-93 (1982).
30. J. Petr, V. Maier, J. Horáková, J. Ševcík and Z. Stránský, Journal of separation science **29** (18), 2705-2715 (2006).
31. G. Garcia-Schwarz, A. Rogacs, S. S. Bahga and J. G. Santiago, Journal of Visualized Experiments (61) (2012).
32. P. Gebauer and P. Boček, Electrophoresis **18** (12-13), 2154-2161 (1997).
33. P. Gebauer and P. Boček, Electrophoresis **21** (18), 3898-3904 (2000).
34. P. Gebauer and P. Boček, Electrophoresis **23** (22-23), 3858-3864 (2002).
35. P. Gebauer, Z. Malá and P. Boček, Electrophoresis **28** (1-2), 26-32 (2007).
36. P. Gebauer, Z. Malá and P. Boček, Electrophoresis **30** (1), 29-35 (2009).
37. P. Gebauer, Z. Malá and P. Boček, Electrophoresis **32** (1), 83-89 (2011).
38. Z. Malá, P. Gebauer and P. Boček, Electrophoresis (2012).
39. J. G. Shackman and D. Ross, Electrophoresis **28** (4), 556-571 (2007).
40. C. Ivory, Separation Science and Technology **35** (11), 1777-1793 (2000).
41. R. T. Kelly and A. T. Woolley, Journal of separation science **28** (15), 1985-1993 (2005).
42. M. M. Meighan, S. J. R. Staton and M. A. Hayes, Electrophoresis **30** (5), 852-865 (2009).

43. C. A. Vyas, P. M. Flanigan and J. G. Shackman, Bioanalysis **2** (4), 815-827 (2010).
44. F. Kohlrausch, Annalen der Physik **298** (10), 209-239 (1897).
45. V. Hruška and B. Gaš, Electrophoresis **28** (1-2), 3-14 (2007).
46. T. K. Khurana and J. G. Santiago, Analytical Chemistry **80** (1), 279-286 (2007).
47. R. D. Chambers and J. G. Santiago, Analytical Chemistry **81** (8), 3022-3028 (2009).
48. T. K. Khurana and J. G. Santiago, Analytical Chemistry **80** (16), 6300-6307 (2008).
49. D. Kaniansky, M. Masár, J. Bielčiková, F. Iványi, F. Eisenbeiss, B. Stanislawski, B. Grass, A. Neyer and M. Jöhnck, Analytical Chemistry **72** (15), 3596-3604 (2000).
50. M. Bercovici, C. M. Han, J. C. Liao and J. G. Santiago, Proceedings of the National Academy of Sciences **109** (28), 11127-11132 (2012).
51. D. Bottenus, T. Z. Jubery, P. Dutta and C. F. Ivory, Electrophoresis **32** (5), 550-562 (2011).
52. S. S. Bahga and J. G. Santiago, Analyst **138** (3), 735-754 (2013).
53. A. A. Kazarian, E. F. Hilder and M. C. Breadmore, Journal of separation science **34** (20), 2800-2821 (2011).
54. W. S. Koegler and C. F. Ivory, Journal of Chromatography A **726** (1–2), 229-236 (1996).
55. W. S. Koegler and C. F. Ivory, Biotechnology Progress **12** (6), 822-836 (1996).
56. J. Liu, X. Sun, P. B. Farnsworth and M. L. Lee, Analytical Chemistry **78** (13), 4654-4662 (2006).
57. Q. Wang, S.-L. Lin, K. F. Warnick, H. D. Tolley and M. L. Lee, Journal of Chromatography A **985** (1–2), 455-462 (2003).
58. D. N. Petsev, G. P. Lopez, C. F. Ivory and S. S. Sibbett, Lab on a Chip **5** (6), 587-597 (2005).
59. R. D. Greenlee and C. F. Ivory, Biotechnology Progress **14** (2), 300-309 (1998).
60. D. W. Inglis, E. M. Goldys and N. P. Calander, Angewandte Chemie International Edition **50** (33), 7546-7550 (2011).
61. Z. Huang and C. F. Ivory, Analytical Chemistry **71** (8), 1628-1632 (1999).
62. N. I. Tracy, Z. Huang and C. F. Ivory, Biotechnology Progress **24** (2), 444-451 (2008).
63. N. I. Tracy and C. F. Ivory, Electrophoresis **29** (13), 2820-2827 (2008).
64. J. M. Burke, Z. Huang and C. F. Ivory, Analytical Chemistry **81** (19), 8236-8243 (2009).
65. S. M. Kim, G. J. Sommer, M. A. Burns and E. F. Hasselbrink, Analytical Chemistry **78** (23), 8028-8035 (2006).
66. Z. Ge, C. Yang and G. Tang, International Journal of Heat and Mass Transfer **53** (13–14), 2722-2731 (2010).

67. G. J. Sommer, S. M. Kim, R. J. Littrell and E. F. Hasselbrink, Lab Chip **7** (7), 898-907 (2007).
68. M. Akbari, M. Bahrami and D. Sinton, Microfluidics and Nanofluidics **12** (1), 221-228 (2012).
69. K. M. Balss, D. Ross, H. C. Begley, K. G. Olsen and M. J. Tarlov, Journal of the American Chemical Society **126** (41), 13474-13479 (2004).
70. S. J. Hoebel, K. M. Balss, B. J. Jones, C. D. Malliaris, M. S. Munson, W. N. Vreeland and D. Ross, Analytical Chemistry **78** (20), 7186-7190 (2006).
71. M. Shariatgorji, J. Astorga-Wells and L. Ilag, Anal Bioanal Chem **399** (1), 191-195 (2011).
72. J. Astorga-Wells, H. Jörnvall and T. Bergman, Analytical Chemistry **75** (19), 5213-5219 (2003).
73. S. Vollmer, J. Astorga-Wells, T. Bergman and H. Jörnvall, International Journal of Mass Spectrometry **259** (1–3), 73-78 (2007).
74. http://www.epizell.com/service_electrocapture.html.
75. R. Dhopeshwarkar, D. Hlushkou, M. Nguyen, U. Tallarek and R. M. Crooks, Journal of the American Chemical Society **130** (32), 10480-10481 (2008).
76. R. K. Perdue, D. R. Laws, D. Hlushkou, U. Tallarek and R. M. Crooks, Analytical Chemistry **81** (24), 10149-10155 (2009).
77. K. N. Knust and R. M. Crooks, Lab on a Chip (2012).
78. T. A. Zangle, A. Mani and J. G. Santiago, Chemical Society Reviews **39** (3), 1014-1035 (2010).
79. S. J. Kim, Y. A. Song and J. Han, Chemical Society Reviews **39** (3), 912-922 (2010).
80. Q. Pu, J. Yun, H. Temkin and S. Liu, Nano Letters **4** (6), 1099-1103 (2004).
81. R. B. Schoch, J. Han and P. Renaud, Reviews of Modern Physics **80** (3), 839 (2008).
82. J. H. Lee, Y.-A. Song, S. R. Tannenbaum and J. Han, Analytical Chemistry **80** (9), 3198-3204 (2008).
83. J. H. Lee, B. D. Cosgrove, D. A. Lauffenburger and J. Han, Journal of the American Chemical Society **131** (30), 10340-10341 (2009).
84. A. Sarkar and J. Han, Lab on a Chip **11** (15), 2569-2576 (2011).
85. Y.-C. Wang and J. Han, Lab on a Chip **8** (3), 392-394 (2008).
86. L. F. Cheow and J. Han, Analytical Chemistry **83** (18), 7086-7093 (2011).
87. J. H. Lee and J. Han, Microfluidics and Nanofluidics 9 (4), 973-979 (2010).
88. S. H. Ko, S. J. Kim, L. F. Cheow, L. D. Li, K. H. Kang and J. Han, Lab on a Chip 11 (7), 1351-1358 (2011).
89. C. Wang, J. Ouyang, D.-K. Ye, J.-J. Xu, H.-Y. Chen and X.-H. Xia, Lab on a Chip 12 (15), 2664-2671 (2012).

90. S. J. Kim, S. H. Ko, K. H. Kang and J. Han, Nature Nanotechnology 5 (4), 297-301 (2010).
91. J. H. Lee, Y.-A. Song and J. Han, Lab on a Chip 8 (4), 596-601 (2008).
92. S. H. Ko, Y.-A. Song, S. J. Kim, M. Kim, J. Han and K. H. Kang, Lab on a Chip 12 (21), 4472-4482 (2012).
93. C. H. Kuo, J. H. Wang and G. B. Lee, Electrophoresis 30 (18), 3228-3235 (2009).
94. J. Quist B. Trietsch, P. Vulto, T Hankemeier (submitted).
95. T. K. Khurana and J. G. Santiago, Lab Chip 9 (10), 1377-1384 (2009).
96. H. Lin, J. G. Shackman and D. Ross, Lab on a Chip 8 (6), 969-978 (2008).
97. J. Astorga-Wells, S. Vollmer, T. Bergman and H. Jörnvall, Analytical Chemistry 79 (3), 1057-1063 (2007).
98. D. Hlushkou, R. K. Perdue, R. Dhopeshwarkar, R. M. Crooks and U. Tallarek, Lab Chip 9 (13), 1903-1913 (2009).
99. D. R. Laws, D. Hlushkou, R. K. Perdue, U. Tallarek and R. M. Crooks, Analytical Chemistry 81 (21), 8923-8929 (2009).
100. E. Sheridan, D. Hlushkou, K. N. Knust, U. Tallarek and R. M. Crooks, Analytical Chemistry 84 (17), 7393-7399 (2012).
101. J. Quist, K. G. H. Janssen, P. Vulto, T. Hankemeier and H. J. van der Linden, Analytical Chemistry 83 (20), 7910-7915 (2011).
102. J. Quist, P. Vulto, H. van der Linden and T. Hankemeier, Analytical Chemistry 84 (21), 9065-9071 (2012).
103. A. Rogacs, Y. Qu and J. G. Santiago, Analytical Chemistry (2012).
104. R. K. Anand, E. Sheridan, D. Hlushkou, U. Tallarek and R. M. Crooks, Lab Chip 11 (3), 518-527 (2010).
105. E. Sheridan, K. N. Knust and R. M. Crooks, Analyst 136 (20), 4134-4137 (2011).
106. V. Shkolnikov, S. S. Bahga and J. G. Santiago, Physical Chemistry Chemical Physics (2012).
107. G. Bruchelt, M. Buedenbender, K.-H. Schmidt, B. Jopski, J. Treuner and D. Niethammer, Journal of Chromatography A 545 (2), 407-412 (1991).
108. J. Astorga-Wells, T. Bergman and H. Jörnvall, Analytical Chemistry 76 (9), 2425-2429 (2004).
109. C. C. Park, I. Kazakova, T. Kawabata, M. Spaid, R.-L. Chien, H. G. Wada and S. Satomura, Analytical Chemistry 80 (3), 808-814 (2008).
110. J. Astorga-Wells and H. Swerdlow, Analytical Chemistry 75 (19), 5207-5212 (2003).
111. G. Kaigala, M. Bercovici, M. Behnam, D. Elliott, J. Santiago and C. Backhouse, Lab on a Chip 10 (17), 2242-2250 (2010).